

MeV arise from: (a) the pion mean free path to be used in the final-state interaction calculations, and (b) the single nucleon amplitude $Af = Zf_p + Nf_n$. Conversely, this means that the photoproduction of neutral pions from complex nuclei could be used as a means of investigating the interactions of pions with nucleons and nuclear matter. If the production amplitudes are determined by other methods, the mean free path in nuclear matter can be obtained. If, on the other hand, a reliable estimate of the mean free path is obtained from measurements of absorption of positive and negative pions by complex nuclei, the proton and neutron amplitudes f_p and f_n can be calculated from the π^0 photoproduction cross sections of nuclei with different Z -to- N ratios.

ACKNOWLEDGMENTS

It is a pleasure to thank Dr. R. F. Christy for suggesting the problem and for his continued interest, and Dr. H. A. Weidenmüller for a number of stimulating discussions on some of the finer details. The author is also indebted to the Standard Vacuum Oil Company (South Africa) for generous financial support during the four years at the California Institute of Technology. The numerical calculations were performed on the IBM 709 computer of the Graduate School of Business Administration, University of California at Los Angeles. Most of this article was written while the author was at the Argonne National Laboratory, Argonne, Illinois, on an overseas tour of duty for the South African Atomic Energy Board.

Analysis of $(p,2p)$ Angular Correlation Experiments*

K. L. LIM†

Department of Mathematical Physics, University of Adelaide, Adelaide, South Australia

AND

I. E. MCCARTHY

*Department of Mathematical Physics, University of Adelaide, Adelaide, South Australia
and Department of Physics, University of California, Davis, California*

(Received 14 October 1963)

$(p,2p)$ angular correlations for various p -shell nuclei are analyzed in the distorted-wave Born approximation with simple shell-model assumptions for the struck particle. The object is to define the limits on the information that can be obtained about nuclear structure from present experiments and to suggest how experiments should be improved. It is found that a simple shell-model wave function for the struck particle can be quite well defined by fitting present experimental data but that the choice of optical-model parameters is highly ambiguous. The ambiguity extends to the determination of the effective two-body potential and the necessity for configuration mixing. The rms radius of the proton distribution obtained from $(p,2p)$ curve fitting agrees well with that obtained from electron scattering. The primary need is for better energy and angular resolution.

1. INTRODUCTION

THE first $(p,2p)$ experiments¹ were performed with very high-energy (340-MeV) protons. The distribution of momentum transfer to the residual nucleus was measured by measuring either the angular correlation for a given energy sharing between the emitted protons or the energy distribution at fixed angles. As a first approximation the momentum transfer was regarded as being due only to the motion of the struck particle. The momentum-transfer distribution was

equated with the momentum distribution of nucleons in the nucleus.

It was suggested by Eisberg² that a measurement of the angular correlation between two medium-energy nucleons emitted in time coincidence in a direct interaction might provide a sensitive test of the validity of the assumption that an incident nucleon collides with a single nucleon in the nuclear surface at intermediate energies.

Angular correlations in $(p,2p)$ experiments were measured by Cohen,³ and Griffiths and Eisberg.⁴ In Cohen's experiment not enough data were obtained on the angular correlation for a significant determination of its characteristics. The major effort was expended on

* Supported by the Australian Atomic Energy Commission, the Australian Institute for Nuclear Science and Engineering, and the U. S. Atomic Energy Commission.

† Present address: University of Malaya, Kuala Lumpur, Malaya.

¹ O. Chamberlain and E. Segré, *Phys. Rev.* **87**, 81 (1952); J. B. Cladis, W. N. Hess, and B. J. Moyer, *ibid.* **87**, 425 (1952); P. A. Wolf, *ibid.* **87**, 434 (1952); J. M. Wilcox and B. J. Moyer, *ibid.* **99**, 875 (1955).

² R. M. Eisberg, University of California Radiation Laboratory Report UCRL 2240, 1953 (unpublished).

³ B. L. Cohen, *Phys. Rev.* **108**, 768 (1957).

⁴ R. J. Griffiths and R. M. Eisberg, *Nucl. Phys.* **12**, 225 (1959).

measuring the energy distributions of the emitted protons. Griffiths and Eisberg managed to obtain just enough data to observe a significant angular correlation structure for 40-MeV incident protons with a peak near 90° as would be expected from the two-body collision mechanism. This was done at the expense of energy resolution and no knowledge of the state of the struck particle could be inferred from the experiment. Both these experiments used targets in the Cu, Ni region of the periodic table.

Tyrén, Maris, and Hillman⁵ resolved the summed energy spectrum of the emitted protons in experiments on p -shell nuclei using 185-MeV incident protons. Two groups were obtained in the spectrum corresponding to protons knocked out of the s shell and the p shell.

Gooding and Pugh⁶ resolved p -state events from ($p, 2p$) experiments on C^{12} and measured the angular correlation. This was also done by Anderson, McKenzie, and Wilkinson⁷ using a bubble chamber.

Angular correlations for resolved energy groups⁸ have been recently measured for various light nuclei by Garron *et al.* at 155 MeV, Gottschalk and Strauch at 158 MeV, Tibell *et al.* at 180 MeV and Tyrén *et al.* at 440 MeV. These measurements have all been made for the case of final protons coplanar with the incident proton, making equal angles with the incident direction and with approximately equal energy. Although this method observes a rather restricted region of phase space, it is easy to analyze theoretically.

The different motivations for ($p, 2p$) experiments have been reflected in different methods of analysis. In the early high-energy experiments, the chief interest was in getting some information about the over-all nucleon-momentum distribution in nuclei. It was found to correspond quite closely to the one given by the shell model when analyzed using the impulse approximation and representing the incident and outgoing particles by plane waves.

In the 40-MeV experiment of Griffiths and Eisberg, the object was to study the reaction mechanism. Analysis by McCarthy, Jezak, and Kromminga⁹ showed that the reaction took place predominantly in the nuclear surface. Because of this fact, these authors made a classical separation of the momentum-transfer

distribution into momentum transfer due to the motion of the struck particle and momentum transfer due to distortion of the wave functions in the entrance and exit channels. The latter was represented as a first approximation by a constant momentum. It was shown that in this approximation, at 40 MeV, distortion is as much responsible for the momentum transfer as the motion of the struck particle. This approach was subsequently used by Anderson, McKenzie, and Wilkinson⁷ and Garron *et al.*⁸ as a first-order correction to the assumption that the momentum-transfer distribution is identical with the nucleon-momentum distribution.

The experiment of Griffiths and Eisberg was analyzed by the momentum-distribution approach because the energy and angular resolution was so poor that no information was obtained from a plane-wave Born-approximation calculation with shell-model wave functions performed by Kromminga and McCarthy.¹⁰ A subsequent plane-wave impulse-approximation calculation by Green and Brown¹¹ was equally unsuccessful. At this time a distorted-wave calculation was not feasible with existing computing facilities. The most important feature of angular correlations from separate states is that the peak near 90° resolves into two peaks for states with angular momentum greater than zero.

The experiments in which energy levels were resolved have been analyzed from the point of view of obtaining information about the shell-model wave functions.¹² The impulse approximation has usually been used. The plane-wave approximation for the incident and outgoing protons has been improved by using space-weighting factors calculated semiclassically. The impulse approximation is not valid if the distortion plays a large part in the reaction. It has been shown in these calculations to give the right order of magnitude for the cross sections if the free proton-proton differential cross section is used. The general shape of angular-correlation curves is reproduced, but the fits calculated so far are only qualitative.

Even in the shell-model analyses, the notion of nucleon-momentum distribution has often been used although of course it is only an intermediate step since it is calculated from the wave functions, which are themselves used in the basic momentum-transfer calculation and which turn out to be quite well determined. No reference to momentum distributions is necessary.

There is a large body of opinion that the nucleon-momentum distribution is not a useful concept in relation to ($p, 2p$) experiments. Baker, McCarthy, and

⁵ H. Tyrén, Th. A. J. Maris, and P. Hillman, *Nuovo Cimento* **6**, 1507 (1957); H. Tyrén, P. Hillman, and Th. A. J. Maris, *Nucl. Phys.* **7**, 10 (1958); P. Hillman, H. Tyrén, and Th. A. J. Maris, *Phys. Rev. Letters* **5**, 107 (1960).

⁶ T. J. Gooding and H. G. Pugh, *Nucl. Phys.* **18**, 46 (1960).

⁷ D. Anderson, J. McKenzie, and D. H. Wilkinson, *Proceedings of the International Conference on Nuclear Structure, Kingston, 1960* (North-Holland Publishing Company, Amsterdam, 1960), p. 319.

⁸ J. P. Garron, J. C. Jacmart, M. Riou, C. Ruhla, J. Teillac, and K. Strauch, *Nucl. Phys.* **37**, 126 (1962); and *Phys. Rev. Letters* **7**, 172 (1961); G. Tibell, O. Sundberg, and U. Miklavzic, *Phys. Letters* **1**, 172 (1962); **2**, 100 (1962); H. Tyrén, S. Kullander, and R. Ramachandran, in *Proceedings of the International Symposium on Direct Interactions and Nuclear Reaction Mechanisms, Padua, 1962* (Gordon and Breach, New York, 1963); B. Gottschalk and K. Strauch, *Phys. Rev.* **120**, 1005 (1960).

⁹ I. E. McCarthy, E. V. Jezak, and A. J. Kromminga, *Nucl. Phys.* **12**, 274 (1959).

¹⁰ A. J. Kromminga and I. E. McCarthy, University of Minnesota Linear Accelerator Laboratory Annual Progress Report, November 1958 (unpublished).

¹¹ A. M. Green and G. E. Brown, *Nucl. Phys.* **18**, 1 (1960).

¹² G. Jacob, in *Proceedings of the International Symposium on Direct Interactions and Nuclear Reaction Mechanisms, Padua, 1962* (Gordon and Breach, New York, 1963); T. Berggren and G. Jacob (to be published); A. Johansson and Y. Sakamoto, *Nucl. Phys.* **42**, 631 (1963).

Porter¹³ emphasized that the momentum distribution is not even defined experimentally without reference to the method of measurement. The method of measurement affects the distribution obtained. Partial localization of the reaction to the nuclear surface contributes high-momentum components. This has been emphasized by Benioff and McCarthy.¹⁴

It has been further pointed out by Gottfried¹⁵ that even the distribution of momentum transfers predicted by the distorted-wave Born approximation (DWBA) is not reliable since it does not take account of three-body collisions. It can be expected to predict the very high-momentum part of the momentum-transfer spectrum wrongly, so it is not useful for considerations of nuclear-momentum distribution that go beyond the shell model.

The concept of nucleon-momentum distribution in relation to $(p,2p)$ experiments is therefore at best an intermediate idea useful only when better calculations cannot be performed. It does not bear any useful relationship to the "actual nucleon-momentum distribution" which is the square of the Fourier transform of the wave function of the nucleus.

It may be concluded, however, that $(p,2p)$ is a very good tool for investigating shell-model wave functions. The question of just *how* good can be answered by a distorted-wave Born-approximation calculation. Such a calculation has been reported by the present authors¹⁶ for 155-MeV protons on C¹². The present work reports a more detailed investigation.

The approximations used are discussed in Sec. 2. The method of computation is outlined in Sec. 3. The effects of the parameters on the angular-correlation curves are studied in Sec. 4. Comparison with experimental data is made in Sec. 5. The effect of asymmetric energy sharing in the final state is shown in Sec. 6. The amount of surface localization is investigated in Sec. 7.

2. DISCUSSION OF APPROXIMATIONS

The shell-model properties of the nucleus are taken into account with the extreme single-particle model. We assume the reaction to proceed via a clean knock-out process that leaves the rest of the nucleus unaffected. If the knocked-out proton was originally in the outermost shell, we assume the residual nucleus to be left in its ground state. This assumption implies that the fractional-parentage coefficient to the ground state is predominant. We can expect this assumption to be good if the nearest excited state is several MeV above the ground state. Due to the residual nucleus having to

rearrange itself into the size and symmetry of its ground state, there will be some rearrangement energy. We suppose this rearrangement energy to be negligible.

For an inner-shell nucleon, the residual nucleus will be left in a highly excited state and rearrangement will take place. If the decay time of that excited state is much longer than the time taken for the nucleons to leave the nucleus, then that excited state can be regarded as the final state for the purpose of computing the matrix element. For simplicity we shall assume that this is the case.

For outer-shell protons with the ground-state assumption for the residual nucleus, the initial and final nuclear spins are completely determined. To obtain these spin values we have used the $j-j$ coupling model for nuclei. This assumes the knocked-out proton initially had an intrinsic spin which was coupled to its orbital-angular momentum. For consistency then, we shall assume all the free protons to have intrinsic spins but that these spins are not coupled to their orbital angular momenta. This assumption implies the neglect of spin-orbit forces in the optical-model potential. In the case of s -state protons, the residual nucleus is left in a highly excited state with spin J' which is not measured. If, however, the initial nuclear spin J is zero, then J' is completely determined by the Clebsch-Gordan coefficients ($J' = \frac{1}{2}$). If J' is not zero the selection rules admit two values for J' , namely $J' = J \pm \frac{1}{2}$.

The radial wave function for each case is calculated in a finite square well of radius a , depth V_B , using as the binding energy the observed separation energy. The radii for the square wells for the s and p states are determined to some extent phenomenologically, but the condition that the rms radius for the charge distribution must be equal to the value obtained by electron scattering¹⁷ is kept in mind.

In this approximation the differential cross section is given by

$$\begin{aligned} d^3\sigma/d\Omega_L d\Omega_R dE_L = & \frac{2\pi}{\hbar} \frac{m_0}{\hbar k_0} \frac{2m_0^3}{(2\pi\hbar)^6} \frac{N}{(E_L E_R)^{1/2}} \frac{N}{2J+1} \\ & \times \sum_{MM'm} C(J'jJ, M'M-M')^2 \\ & \times C(Lsj, mM-M'-m)^2 |M_L^m|^2. \quad (1) \end{aligned}$$

J' , j , and J are the angular momenta of the residual nucleus, the struck particle and the initial nucleus M' , m and M are the corresponding magnetic quantum numbers, L and s are the orbital angular momentum and spin of the struck particle. m_0 is the proton mass. N is the number of protons in the relevant shell-model state. C is a Clebsch-Gordan coefficient.

In the distorted-wave Born approximation

$$\begin{aligned} M_L^m(\theta) = & \int d^3r_1 d^3r_2 \chi^{(+)}(\mathbf{k}_0, \mathbf{r}_1) \chi^{(-)*}(\mathbf{k}_L, \mathbf{r}_1) \\ & \times \chi^{(-)*}(\mathbf{k}_R, \mathbf{r}_2) \psi_L^m(\mathbf{r}_2) v(\mathbf{r}_1 - \mathbf{r}_2). \quad (2) \end{aligned}$$

¹³ G. A. Baker, Jr., I. E. McCarthy, and C. E. Porter, Phys. Rev. **120**, 254 (1960).

¹⁴ P. A. Benioff, Phys. Rev. **119**, 324 (1960); I. E. McCarthy, *Proceedings of the International Symposium on Direct Interactions and Nuclear Reaction Mechanisms, Padua, 1962* (Gordon and Breach, New York, 1963).

¹⁵ K. Gottfried, Ann. Phys. (N. Y.) **21**, 1 (1963).

¹⁶ K. L. Lim and I. E. McCarthy, Phys. Rev. Letters **10**, 529 (1963).

¹⁷ R. Herman and R. Hofstadter, *High-Energy Electron Scattering Tables* (Stanford University Press, Stanford, California, 1960).

$\chi^{(+)}$ and $\chi^{(-)*}$ are optical-model wave functions for ingoing and outgoing particles. \mathbf{k}_0 , \mathbf{k}_L , and \mathbf{k}_R are the momenta of the incident proton and the protons scattered to the left and right, respectively. θ is the angle between \mathbf{k}_L or \mathbf{k}_R and \mathbf{k}_0 in the center-of-mass system. Optical-model parameters are V_0 , W_0 , r_0 , and b for the initial state and V_1 , W_1 , r_1 , and b for the final state describing Eckart form factors. $v(\mathbf{r}_1-\mathbf{r}_2)$ is the effective two-body potential in the region of interaction.

If the optical-model wave functions are approximated by plane waves, the matrix element factorizes in the following way.

$$M_L^m = \int d^3r' e^{i\mathbf{k}_0 \cdot \mathbf{r}'} v(\mathbf{r}') e^{-i\mathbf{k}_L \cdot \mathbf{r}'} \int d^3r e^{i\mathbf{K} \cdot \mathbf{r}} \psi_L^m(\mathbf{r}), \quad (3)$$

where \mathbf{K} is the momentum transfer. The final factor is the matrix element in the case

$$v(\mathbf{r}_1-\mathbf{r}_2) = V_s \delta(\mathbf{r}_1-\mathbf{r}_2).$$

This is multiplied by the Fourier transform of the two-body potential. If, at the appropriate energy, the square of this Fourier transform is replaced by the free proton-proton differential cross section for 90° scattering, we have the impulse approximation. The factorization is not exact in the case of distorted waves. The analyses of Ref. 12 have used an approximation for the distortion in which it is exact.

In the present work we have set $v(\mathbf{r}_1-\mathbf{r}_2)$ equal to $V_s \delta(\mathbf{r}_1-\mathbf{r}_2)$. V_s is the only free parameter in the theory. It is worth examining the cases of Gaussian and Yukawa shape for $v(\mathbf{r}_1-\mathbf{r}_2)$ in the plane-wave case. In both cases large separation angles are suppressed with respect to small ones. This phenomenon is observed in the experimental p -state angular correlations. In the case of 155-MeV incident protons, the use of a reasonable potential range with a Gaussian potential gives a ratio of left to right peak larger than 5. The use of a Yukawa potential gives a ratio of about 7/4. Experimentally the ratio is between 1 and 2.

A ratio of left to right peak greater than 1 is also a result of distortion. Because of this ambiguity we have decided to ignore the effect of finite range and not to use the peak ratio as a sensitive criterion of fitting. The order of accuracy of the experiments does not warrant a better approximation.

The optical-model wave functions are calculated using Eckart form factors for both the real and imaginary parts of the potential. Spin-orbit coupling is neglected. The normal method of calculating optical-model wave functions requires the conversion of a two-body problem into a one-body problem. For the entrance channel in ($p, 2p$) this is sufficient. The exit channel, however, requires the solution of a three-body problem. Since we need to use the normal optical model for computational reasons, we have made the following approximation for the final state.

After separating off the equation of motion of the center of mass, the two final-state particles are described by

$$\left[\frac{1}{2\mu} \nabla_L^2 + \mathcal{U}_L - \frac{1}{2\mu} \nabla_R^2 + \mathcal{U}_R - \frac{1}{A} \nabla_L \cdot \nabla_R \right] \psi_{LR} = E \psi_{LR}. \quad (4)$$

The coordinate systems for the left and right particles relative to the residual nucleus are respectively denoted by L , R . E is the total energy in the center-of-mass system. \mathcal{U}_L and \mathcal{U}_R are the optical-model potentials. $\mu = A/(A+1)$ where A is the mass number of the residual nucleus.

If the term in $1/A$ is treated as a perturbation, then to first order ψ_{LR} is separable and $\nabla_L \cdot \nabla_R$ can be replaced by its eigenvalue $-\mathbf{p}_L^\dagger \cdot \mathbf{p}_R^\dagger / \hbar^2$. \mathbf{p}_L^\dagger and \mathbf{p}_R^\dagger are the momenta conjugate to the relative positions of the left and right protons.

In this approximation, the one-body Schrödinger equation for the left proton, for example, is

$$\left(-\frac{1}{2\mu} \nabla_L^2 + \mathcal{U}_L \right) \psi_L = \left[\frac{1}{2} \left(\frac{1+\alpha}{1+2\alpha} E_{\text{lab}} + Q \right) \times \left\{ 1 - \frac{\alpha[(4\alpha^2+4\alpha+2) \cos^2\theta - 1]}{(1+\alpha)^2(1+2\alpha \cos^2\theta)} \right\} \right] \psi_L. \quad (5)$$

E_{lab} is the incident energy in the laboratory system. Q is the Q value for the reaction $\alpha=1/A$. If η is the measured energy difference between the two final particles in the laboratory system and E_{lab} , then to first order in α ,

$$Q = \eta(1+2\alpha \cos^2\theta) + \alpha E_{\text{lab}}(1+2 \cos^2\theta - 2\sqrt{2} \cos\theta). \quad (6)$$

It will be noticed that the energy used in the final-state Schrödinger equation depends on θ . This is awkward from the computational point of view because it requires one run for each point in the angular correlation. This point is discussed further in Sec. 5.

Other physical approximations made are the neglect of relativistic effects and the neglect of the Coulomb repulsion between the protons in the final state. These approximations are expected to involve shifts of the angular-correlation curve of about 1° which is marginally significant in comparison with the experimental angular resolution.

3. METHOD OF COMPUTATION

In the case in which the outgoing protons are coplanar with the incident direction and make equal angles with it, the matrix element may be written

$$M_L^m(k_0, k_L, k_R, \theta) = \left(\frac{2L+1}{4\pi} \right)^{1/2} (4\pi)^2 \sum_{\nu\nu'} I^m_{\nu\nu'L}(\theta) \times R_{\nu\nu'L}(k_0, k_L, k_R), \quad (7)$$

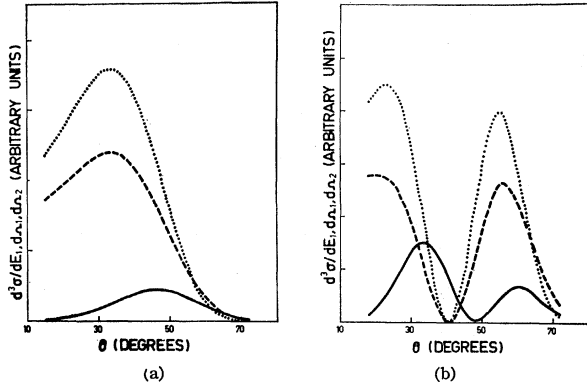


FIG. 1. Variation of the square-well radius a for (a) the s -state angular correlation and (b) the p -state angular correlation for the case $C^{12}(p,2p)B^{11}$ at 155 MeV. The continuous curve is the standard run. The dashed and dotted curves are for zero potential and $a=2.4$ and 3.0 F in Fig. 1(a) and 2.8 and 3.5 F in Fig. 1(b).

where

$$I_{l'l''l}^{m'l''m}(\theta) = i^{l-l''} (2l+1) \left(\frac{4\pi}{2l'+1} \right)^{1/2} \left(\frac{4\pi}{2l''+1} \right)^{1/2} \times \sum_{np} (-1)^p C(nLl'',00) C(nLl',-pm) Y_{l',m-p}(\Omega_R) \times C(nl'',00) C(nl',p0) Y_{l',p}(\Omega_L), \quad (8)$$

and

$$R_{l'l''l}(k_0, k_L, k_R) = \int f_l(k_0 r) f_{l'}(k_L r) f_{l''}(k_R r) \times u_L(r) r^2 dr. \quad (9)$$

Ω_L and Ω_R are the angular coordinates of the left and right proton, respectively. The azimuthal angles are set, respectively, at 0 and π .

The expression (1) for the angular correlation was coded in Fortran for the IBM 7090. The program consists of two separate codes—one for s -state and one for p -state protons, and each of them is in two parts. The first part computes the parameter independent factors $I_{l'l''l}^{m'l''m}(\theta)$ of Eq. (7) for fixed maximum values of l , l' , and l'' and fixed values of θ , then stores these factors on magnetic tape. The second part computes the radial optical-model and bound-state wave functions for a given set of parameters, and then computes the angular correlation via Eq. (7). The maximum values of l , l' , and l'' have been taken to be 11 , 8 , and 8 corresponding approximately to $kR+3$ for the free protons in the reaction $155\text{-MeV } C^{12}(p,2p)B^{11}$. This implies that the code is restricted to $(p,2p)$ reactions at low or medium energies on light nuclei. However, this restriction is necessary from the point of view of computing time. With these values for the l 's and 30 values of θ , the computation time for the I 's in the case of p -state protons is already 50 min, and increasing each value by just one, approximately doubles the computation time. After this initial 50 min, each angular correlation computation requires only $3\frac{1}{2}$ min of 7090 time. Thus,

TABLE I. Values of the parameters for the standard run.

(1p)	$a=3.5$ F	$V_B=38.4$ MeV	
	$V_0=5.0$ MeV	$W_0=15.0$ MeV	$r_0=1.3$ F
	$V_1=40.0$ MeV	$W_1=10.0$ MeV	$r_1=1.3$ F
(1s)	$a=2.4$ F	$V_B=58.0$ MeV	
	$V_0=5.0$ MeV	$W_0=15.0$ MeV	$r_0=1.3$ F
	$V_1=40.0$ MeV	$W_1=10.0$ MeV	$r_1=1.3$ F

this splitting up of the program makes parameter studies and curve fitting feasible.

The effects on the angular correlation of the optical-model and bound-state parameters are independent of the coordinate system. In this parameter study we have used the center-of-mass system and have introduced an approximation for the energy $E_{c.m.}$ of the outgoing particles. The dependence of $E_{c.m.}$ on the angle at which the protons emerge has been neglected. It is taken to be equal to its value when $\theta=45^\circ$. The parameters that have to be varied are the radius a of the square well generating the bound-state wave function, and the optical-model parameters V_0 , W_0 , r_0 and V_1 , W_1 , r_1 of the incident and outgoing protons, respectively.

The form factors for the real and imaginary parts of the optical potential are taken to be Eckart form factors with the rounding parameter b set equal to 0.65 F. The Coulomb radius is taken to be equal to the nuclear radius. The values of these parameters for the standard run in this study of the $155\text{-MeV } C^{12}(p,2p)B^{11}$ reaction are given in Table I.

A cursory glance at the Figs. 1(a), 1(b), 2(a), 2(b), 3(a), 3(b), 4(a), and 4(b), illustrating the effects of the variations of these parameters will show that they have the same effects on the angular correlations for the s and p states. Thus the following description of the effects should be regarded as applying to both s and p states.

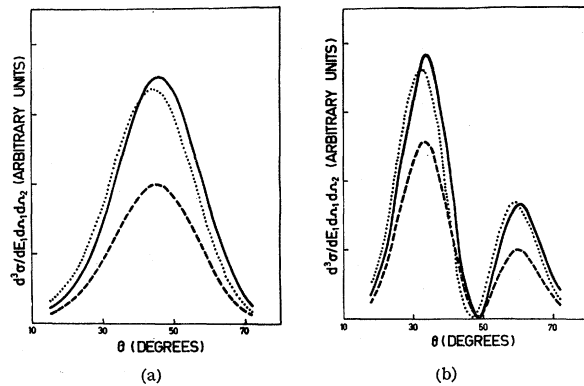


FIG. 2. Variation of the entrance-channel optical-model potentials V_0 , W_0 for (a) the s -state angular correlation and (b) the p -state angular correlation for the case $C^{12}(p,2p)B^{11}$ at 155 MeV. The continuous curve is the standard run. The dashed curve in both cases is for $V_0=5.0$ MeV, $W_0=30.0$ MeV. The dotted curve is for $V_0=20.0$ MeV, $W_0=15.0$ MeV.

For a particular nucleus, the binding energies of the $1s$ and $1p$ protons have been determined experimentally, and thus there is only one independent parameter left to be varied. This parameter is taken to be a , the radius of the square well generating the bound-state wave function. The transcendental equations are first solved for V_B for several values of a and these pairs of values of a and V_B are read in as input parameters in the Fortran program. The effects of the variation of a on the angular correlations can be seen from Figs. 1(a) and 1(b). The optical-model parameters have been set equal to zero. Increasing a has two effects on the cross section. Firstly, it increases the magnitude of the cross section, and secondly, it decreases the over-all width of the curves. In fact, it is the only parameter that has any appreciable effect on the over-all width. It will be seen later that it is this property of a that allows it to be fairly well determined by trying to fit the over-all widths of the experimental data.

It is to be expected that the variation of the parameters of the exit channel will have a larger effect on the angular correlations than the same variation of the parameters of the incident channel, as they determine two outgoing optical-model wave functions. Figures 2(a) and 2(b) show the effects of varying V_0 and W_0 of the incident proton. V_0 has only a small effect on the correlation, and a large increase in V_0 shifts the curves to slightly smaller angles. It also simultaneously slightly decreases the maxima in the curves. W_0 has the expected effect of decreasing the magnitude of the correlation, but the p -state minimum is not raised by any appreciable amount. Figures 3(a) and 3(b) illustrate the effects of varying V_1 and W_1 of the exit channel. The effect of V_1 on the location of the curve is opposite to that of V_0 . Increasing V_1 shifts the curves to larger angles and the shift is quite appreciable. It is found that this effect is very important in locating the theoretical curves properly with respect to the experimental data. As in the case with V_0 , the increasing of V_1 slightly

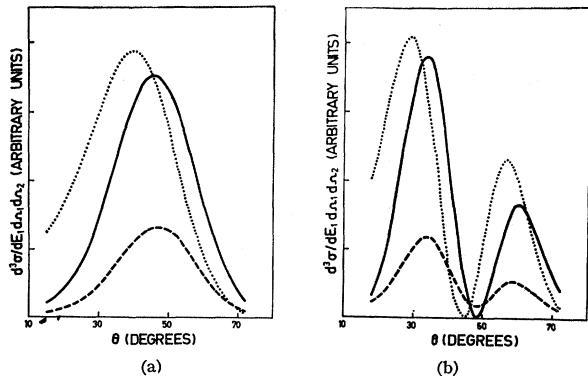


FIG. 3. Variation of the exit-channel optical-model potentials V_1 , W_1 as in Fig. 2. The dashed curve is for $V_1=40.0$ MeV, $W_1=20$ MeV in Fig. 3(a) and $V_1=40.0$ MeV, $W_1=30.0$ MeV in Fig. 3(b). The dotted curve is for $V_1=20.0$ MeV, $W_1=10$ MeV in both cases.

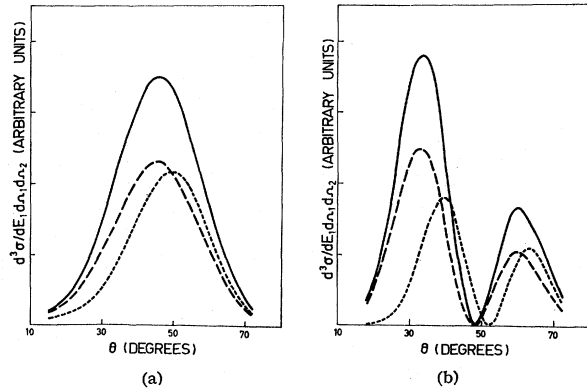


FIG. 4. Variation of the optical-model radius parameters r_0 and r_1 for (a) the s -state angular correlation and (b) the p -state angular correlation for the case $C^{12}(p, 2p)B^{11}$ at 155 MeV. The continuous curve is the standard run. The dashed curve is for $r_0=1.9$ F, $r_1=1.3$ F in both cases. The dotted curve is for $r_0=1.3$ F, $r_1=1.9$ F in both cases.

decreases the maxima in the curves. Increasing W_1 decreases the magnitude of the angular correlation, and also has the very important effect of lifting the p -state minimum appreciably, and thus decreasing the small-angle peak to minimum ratio. This is highly desirable in fitting experimental data where no deep minimum, predicted by the plane-wave Born approximation, is observed.

Lastly there are the nuclear radius parameters r_0 and r_1 to be varied. The nuclear radius is related to $r_0(r_1)$ via $R=r_0 A^{1/3} [r_1(A-1)^{1/3}]$, where A is the mass number of the target nucleus. As the cross section is dependent on the potential volume rather than on the strengths of the potentials only, we expect the effects of the variation of $r_0(r_1)$ to be somewhat equivalent to effects of the simultaneous variations of $V_0(V_1)$ and $W_0(W_1)$. Figures 4(a) and 4(b) illustrate the effects of varying $r_0(r_1)$ and indeed show that the expectation is correct.

The experimental data of Garron *et al.*⁸ that we shall try to fit have an error of approximately 20% in the absolute magnitude of the cross section. The error in the angular resolution is $\pm 2.5^\circ$ and the protons are detected when the energy of one of them is in the range of 60 to 80 MeV, approximately. On account of this error, it is important to decide which of the experimental features are sufficiently well defined to try to reproduce with our theory. The features in the s - and p -state angular correlations that we shall take into account in fitting are: (1) The location of the curve on the θ axis, (2) the over-all width of the curve, (3) the magnitudes of the s - and p -state cross sections. The depth of the minimum and the ratio of the peak heights in the p -state curve are not considered to be sufficiently well defined to fit, but we will show how a reasonable value can be obtained considering the above energy and angular resolution.

Having decided on the experimental features that should be reproduced by the theory, we shall now

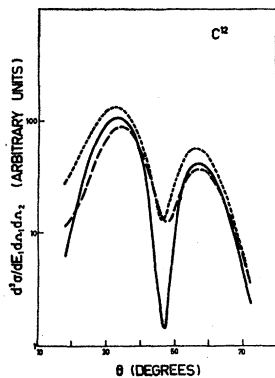


FIG. 5. p -state angular correlations for $C^{12}(p,2p)B^{11}$ at 155 MeV computed with very different values for the optical-model potentials. Curve 1 (full line) $V_0=24$ MeV, $V_1=39$ MeV, $W_0=40$ MeV, $W_1=24$ MeV, curve 2 (dashed line) $V_0=36$ MeV, $V_1=50$ MeV, $W_0=24$ MeV, $W_1=32$ MeV, curve 3 (dotted line) $V_0=12$ MeV, $V_1=30$ MeV, $W_0=24$ MeV, $W_1=32$ MeV.

discuss what information about the values of the parameters we can obtain from curve fitting. It was found in the parameter study that V_0 and V_1 have opposite effects on the location of the curve with respect to the θ axis. Thus the location of the curve is not expected to determine V_0 and V_1 uniquely. In fact, by simultaneously increasing or decreasing both V_0 and V_1 in the appropriate ratio from the values for a fit, we can obtain a range of values for both V_0 and V_1 that will still give a reasonable fit to the data. As both V_0 and V_1 also effect the peak ratio, better experimental data would help in narrowing the range of acceptable values. The Eckart well radius has been taken to be equal to the rms radius of the charge distribution determined from electron scattering by Herman and Hofstadter.¹⁷

The magnitudes of the s -state and p -state curves could be maintained at a fairly constant value by simultaneously increasing W_0 and decreasing W_1 , or vice versa. This discussion shows that $(p,2p)$ angular correlations will not determine the optical-model parameters uniquely but only a fairly wide range of acceptable values.

Figure 5 shows the effects discussed above in the case of C^{12} in the infinite-mass approximation. It is seen that although the curves have very different values of V and W they are not too different. In fact the curves with very different V_0 and V_1 could be made to practically coincide by just varying the W of one of them.

The over-all width of the curve is appreciably affected by only one parameter—the radius a of the square well generating the bound-state wave function. Thus it should be possible to determine a , and hence the rms radius of the charge distribution fairly uniquely by curve fitting.

In Sec. 2 an expression (5) was derived for the energy of each of the outgoing protons as a function of θ , the angle they make with the incident direction. A center-of-mass calculation would require one numerical integration of the radial optical-model equation for each angle. It would be very uneconomical to do this, as the computation time in the infinite-mass approximation is already $3\frac{1}{2}$ min. Since the experiments of Garron *et al.* have been done on light nuclei it would be desirable

TABLE II. Spin assignments for the states used in the calculations.

a state		p state	
Initial state	Final state	Initial state	Final state
$Li^6(1+)$	$He^5(\frac{3}{2}+)$	$Li^6(1+)$	$He^6(\frac{3}{2}-)$
$Li^7(\frac{3}{2}-)$	$He^6(1-)$	$Li^7(\frac{3}{2}-)$	$He^6(0+)$
$B^{10}(3+)$	$Be^5(\frac{3}{2}+)$	$B^{10}(3+)$	$Be^6(\frac{3}{2}-)$
$B^{11}(\frac{3}{2}-)$	$Be^{10}(1-)$	$B^{11}(\frac{3}{2}-)$	$Be^{10}(0+)$
$C^{12}(0+)$	$B^{11}(\frac{3}{2}+)$	$C^{12}(0+)$	$B^{11}(\frac{3}{2}-)$

to try to fit at least one case in the center-of-mass system with reasonable values for the optical potentials. We can expect that to obtain fits, the values of the optical potentials will be different for the center-of-mass and infinite-mass systems. However, we do not attach much significance to the values of the optical potentials on account of the previously mentioned V_0 , V_1 and W_0 , W_1 ambiguities. We will show that the over-all widths will be fairly well reproduced with the same values of a for both systems. This then will be the justification for using the infinite-mass approximation to determine the bound-state parameter a .

Figure 6 shows the angular correlations in the center-of-mass system for the reaction $C^{12}(p,2p)B^{11}$. The angles have been converted to laboratory angles. The curves were obtained by interpolation and extrapolation from three curves computed with energies corresponding to $\theta=30, 45,$ and 60° . Curve 1 was computed using the values of the parameters that gave a reasonable fit to the experimental data in the infinite-mass approximation (see Fig. 8). It should be noted that the curve has been shifted to the left but by decreasing V_0 from 24 MeV to 8 MeV we can relocate the curve properly (curve 2). The most important feature to note is that the over-all width is not appreciably changed. This then justifies our using the infinite-mass approximation for the discussion of the over-all width and magnitudes of the curves.

In the case of s -state protons, the angular correlation is independent of the spin of the residual nucleus. In the following, the spin of the residual nuclei will be taken to be $J-\frac{1}{2}$ for J not equal to zero, although $J+\frac{1}{2}$ is also allowed. For p -state protons, the ground-state to

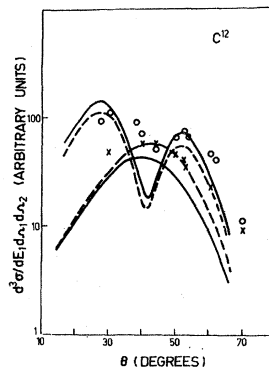


FIG. 6. Angular correlations computed in the center-of-mass system with finite nuclear masses in the case $C^{12}(p,2p)B^{11}$ at 155 MeV. The experimental data are from Garron *et al.*⁸ The circles are for the p state, the crosses for the s state. Curve 1 is the full line for the s state, the dashed line for the p state. Curve 2 is the dashed line for the s state, the full line for the p state. The parameters are given in the text.

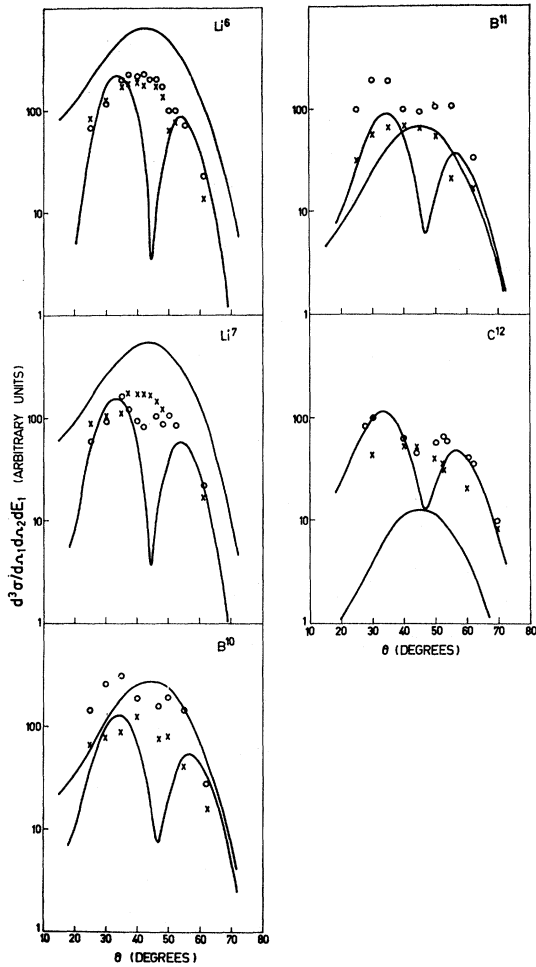


FIG. 7. Angular correlations computed in the infinite-mass approximation using parameters given in Tables III and V compared with the data of Garron *et al.*⁸ The circles indicate the p state, the crosses indicate the s state.

ground-state transition assumption uniquely specifies the nuclear spins involved. The spin assignments are shown in Table II.

There is still one arbitrary parameter in the theory, the strength V_s of the delta-function interaction. The results to be shown have been normalized to the experimental data by adjusting V_s . V_s was fairly constant for all the nuclei investigated and has a value of approximately 800 MeV F^3 . This value is consistent with the values found from fitting $Si^{28}(n,p)$ reactions by Agodi and Schiffrer,¹⁸ and is approximately twice that found from free $n-p$ scattering with a delta-function interaction. However, this value of V_s is not unique and is dependent on the set of W 's used to fit the data. Thus, using this value for V_s , the results shown are in absolute units, i.e., $\mu b/sr^2$ MeV, although in the figures the vertical axes have been expressed in arbitrary units.

¹⁸ A. Agodi and G. Schiffrer, Nucl. Phys. (to be published).

TABLE III. Optical-model parameters computed (Ref. 12) by the method of Kerman, McManus, and Thaler (Ref. 19).

	V_0 (MeV)	W_0 (MeV)	V_1 (MeV)	W_1 (MeV)	$r_0=r_1$ (F)
Li ⁶	8.0	8.0	13.0	11.0	1.95
Li ⁷	10.0	10.0	16.0	13.0	1.9
B ¹⁰	17.0	17.0	28.0	23.0	1.5
B ¹¹	20.0	20.0	32.0	26.0	1.5
C ¹²	24.0	24.0	39.0	32.0	1.35

Berggren and Jacob¹² have computed values for the real and imaginary parts of the optical potential for 170- and 70-MeV protons via the method of Kerman, McManus, and Thaler.¹⁹ With these values for the potentials (Table III) the s -state and p -state angular correlations have been computed for Li⁶, Li⁷, B¹⁰, B¹¹,

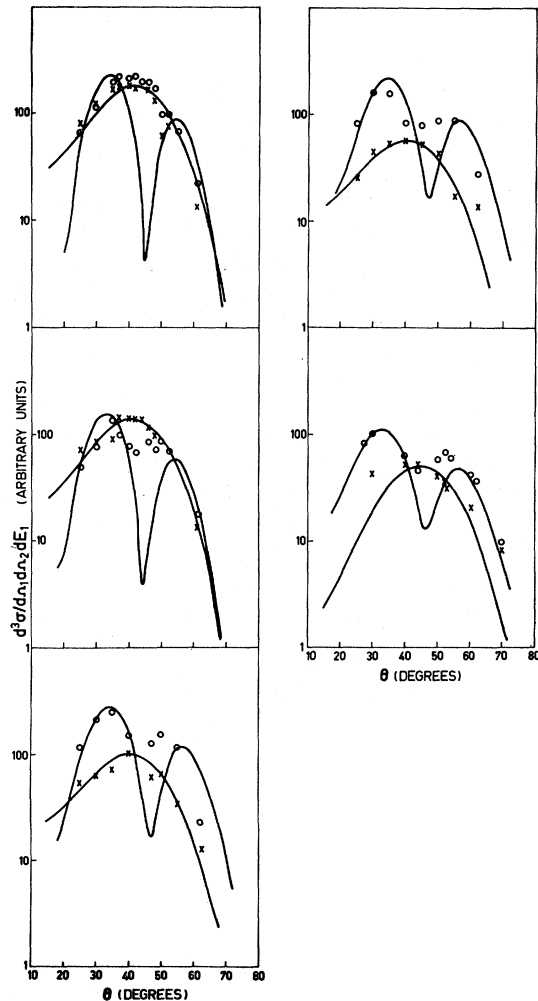


FIG. 8. Angular correlations computed in the infinite-mass approximation using parameters given in Tables IV and V compared with the data of Garron *et al.*⁸ For identification of the curves refer to Fig. 7. The circles indicate the p state, the crosses indicate the s state.

¹⁹ A. K. Kerman, H. McManus, and R. M. Thaler, Ann. Phys. (N. Y.) 8, 551 (1959).

and C^{12} in the infinite-mass approximation. The bound-state parameters (Table V) have been chosen such that the s -state rms radius is approximately the α -particle rms radius, and the p -state rms radius will give roughly the correct charge-distribution rms radius

TABLE IV. Optical-model parameters used for the curves of Fig. 8.

		V_0 (MeV)	W_0 (MeV)	V_1 (MeV)	W_1 (MeV)	$r_0=r_1$ (F)
Li ⁶	s	8.0	8.0	6.0	21.5	1.9
	p	8.0	8.0	13.0	11.0	5
Li ⁷	s	10.0	10.0	8.0	24.0	1.9
	p	10.0	10.0	16.0	13.0	
B ¹⁰	s	17.0	17.0	14.0	35.0	1.5
	p	17.0	17.0	28.0	12.0	
B ¹¹	s	20.0	20.0	16.0	28.0	1.5
	p	20.0	20.0	32.0	12.0	
C ¹²	s	24.0	24.0	39.0	18.0	1.35
	p	24.0	24.0	39.0	32.0	

when correctly weighted with the s -state radius. The computed correlations are shown in Fig. 7. Although the shapes and over-all widths are well reproduced, the absolute magnitudes are not. For Li⁶, Li⁷, B¹⁰, and B¹¹, the s -state magnitudes are too large and the curves are located to the right of the experimental data. In the case of C¹², the curves are properly located, but the s -state magnitude is too small. Thus it is obvious that angular correlations cannot be fitted with equal values of the optical potentials for s - and p -state cases. As the incident energies are the same for both cases it would be sensible to keep the incident-channel parameters equal and vary only the exit channel ones. Figure 8 shows the results obtained using the values of the optical potentials tabulated in Table IV. The values of the bound-state parameters given in Table V reproduce the over-all width very well. It should be noted that the s - and p -state protons had to have potential wells of different radial extension and depth. In general, the wells for the p protons are shallower but extend farther than the s -state wells. The resulting rms radii were then computed and compared with the charge-distribution radii. In Table VI below it is seen that we obtain very good agreement.

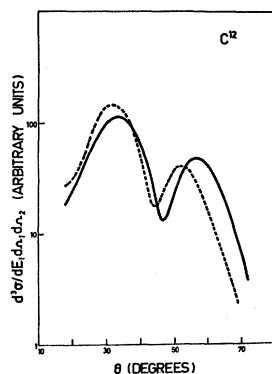


FIG. 9. p -state angular correlation for $C^{12}(p,2p)B^{11}$ at 155 MeV. The full line is for outgoing protons of equal energy. The dashed line is for outgoing protons having an energy difference of 10 MeV.

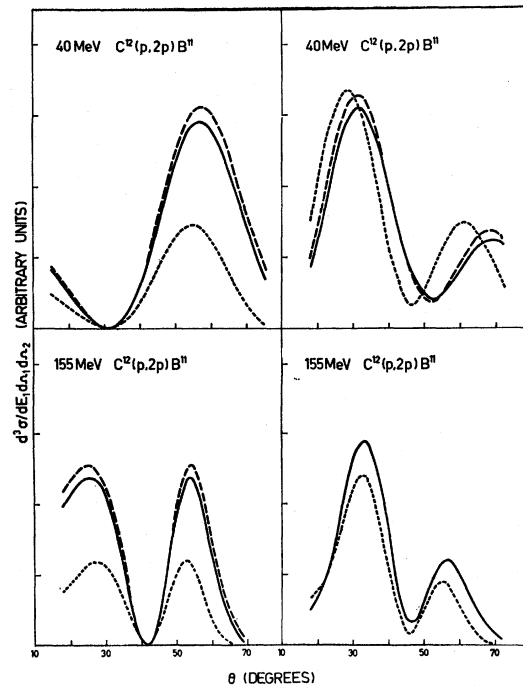


FIG. 10. p -state angular correlations computed with different values of the cutoff radius R_{0c} . The curves on the left are computed with plane waves. The curves on the right are computed with distorted waves using the standard potentials. Curve 1 (full line) is for $R_{0c}=0.0$ F, curve 2 (dashed line) is for $R_{0c}=1.6$ F, curve 3 (dotted line) is for $R_{0c}=2.8$ F.

6. ASYMMETRIC ENERGY SHARING

The p -state correlation is characterized in the plane-wave Born approximation by a zero minimum for zero-momentum transfer. Experimentally this minimum is observed but is very appreciably lifted. Even in the case of symmetric energy sharing between the outgoing protons, we have found that a large enough value of W

TABLE V. Bound-state parameters used in fitting experimental data.

		E_B (MeV)	V_B (MeV)	a (F)	rms radius (F)
Li ⁶	s	22.4	49.8	2.0	1.62
	p	4.0	13.0	5.2	4.41
Li ⁷	s	25.5	49.8	2.2	1.67
	p	10.0	19.8	5.4	4.13
B ¹⁰	s	31.5	55.0	2.3	1.67
	p	7.0	27.5	3.5	3.07
B ¹¹	s	3.40	59.5	2.2	1.6
	p	10.0	28.3	3.8	3.14
C ¹²	s	36.0	58.0	2.4	1.7
	p	16.0	38.4	3.5	2.79

will lift the minimum appreciably. However, symmetric energy sharing is an ideal case, and experimentally it would be expected that a fair proportion of the protons detected would have asymmetric energy sharing. As a lot of importance has been given to observing this

minimum we have here investigated the possibility of asymmetric energy smearing it out.

Figure 9 shows the results with an unequal energy sharing of 10 MeV between the emergent protons. It should be noted that the curve is shifted to the left.

TABLE VI. rms radii of nuclei determined from ($p, 2p$) fits and electron scattering.

	($p, 2p$)	Electron scattering
Li ⁶	2.86	2.83
Li ⁷	2.85	2.83
B ¹⁰	2.60	
B ¹¹	2.64	2.55
C ¹²	2.48	2.42

Thus it is obvious that if we add contributions from asymmetric cases, the final minimum will be lifted and the curve will also be smoother. However, we have not done this because we do not know in what proportion to weight the various contributions.

7. LOCALIZATION OF THE INTERACTION REGION

($p, 2p$) reactions on light nuclei in the incident energy range of 100 to 200 MeV have been taken for granted as occurring throughout the whole nuclear volume. It was generally thought that these reactions were localized to the surface only in the case of low incident energy on medium or heavy nuclei. However, both Lim and McCarthy,²⁰ and Benioff¹⁴ have assumed surface localization even for medium energy on light nuclei. Thus it would be worthwhile investigating the localization of the interaction region.

In this section we shall investigate surface localization by introducing a cutoff radius R_{0c} such that the bound-state wave function is zero for $r < R_{0c}$, viz.,

$$u_L(r) = 0 \quad \text{for } r < R_{0c}.$$

The nucleus under consideration is C¹² for which we have computed p -state correlations for 40- and 155-MeV

incident energies in both the plane-wave and distorted-wave Born approximation. The values of the distorting potentials were taken to be those that fit the C¹² data in the 155-MeV case while, in the 40-MeV case, the values obtained by Bjorklund and Fernbach²¹ from elastic scattering analyses were used. Figure 10 shows the correlations computed for three values of the cutoff radius R_{0c} , namely 0.0, 1.6, and 2.8 F. Figure 11 shows the C¹² s - and p -bound-state wave functions with the cutoff radii marked.

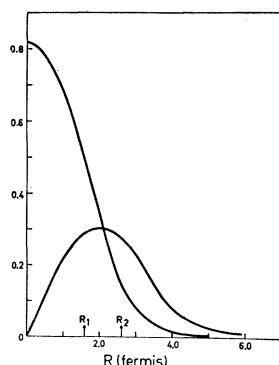
The results are interesting in several aspects. The $R_{0c} = 0.0$ F and $R_{0c} = 1.6$ F correlations are very much the same and for the 155-MeV DWBA case the curves were almost indistinguishable. This implies that the region $r < 1.6$ F (the alpha-particle rms radius), does not contribute much to the matrix element. For $R_{0c} = 2.8$ F the correlations are very different from the correlations computed with no cutoff. This is to be expected as in this case we are cutting off part of the contribution from the nuclear surface region. Thus, if the region outside of the alpha-particle radius of C¹² is considered to be the surface, then it is seen that ($p, 2p$) reactions are indeed localized to the surface. The higher energy results seem to show more surface localization than the lower energy results.

The concept of phase averaging was introduced by Austern²² to explain the localization of nuclear reactions to the nuclear surface. In particular, he applied it to alpha-particle inelastic scattering. However, Amos and McCarthy²³ showed that phase averaging does not significantly reduce the contribution of the interior of the nucleus to the DWBA matrix elements for nucleon inelastic scattering at any energy. The differences in our results for different values of R_{0c} in both the plane-wave and distorted-wave Born approximation seem to be very much the same. Since there is no localization in a plane-wave calculation, we must conclude that the region inside the α -particle radius contributes too little to the overlap integral to have an effect. The localization to the surface is simply that of the p -state wave function.

8. CONCLUSIONS

Distorted-wave Born-approximation analyses of ($p, 2p$) angular correlations should be capable of providing information on certain features of the shell-model wave function. The features that could be determined are possibly the amount of configuration mixing, the shape, radial extension, and depth of the shell-model potential well and the rms radius. However, because of the large angular and energy uncertainties in the experimental data that have so far been measured, we have not been able to obtain such detailed information but

FIG. 11. Bound-state wave functions for C¹² computed using the parameters of Table V. The points R_1 and R_2 indicate the two values of the cutoff parameter R_{0c} used for Fig. 10.



²⁰ K. L. Lim and I. E. McCarthy, in *Proceedings of the International Symposium on Direct Interactions and Nuclear Reaction Mechanisms, Padua, 1962* (Gordon and Breach, New York, 1963).

²¹ F. Bjorklund and S. Fernbach, *Phys. Rev.* **109**, 1295 (1958).

²² N. Austern, *Ann. Phys. (N. Y.)* **15**, 299 (1961).

²³ K. A. Amos and I. E. McCarthy, *Phys. Rev.* **132**, 2261 (1963).

have only determined the rms radii and the depth and radial extension of the square well. The s -state rms radius was found to be approximately equal to that of the alpha particle, and the resultant rms radii for all the nuclei considered, namely Li^6 , Li^7 , B^{10} , B^{11} , and C^{12} , agreed reasonably with the charge distribution rms radii determined from electron scattering. The potential wells for the s -state particles had to have smaller radial extension but greater depth than the wells for the p -state particles. It was found that there were no significant differences in the shape of the cross sections computed from wave functions with the same quantum numbers, binding energy, and rms radius.

It can be expected that $(p,2p)$ angular correlations will not determine the values of the optical potentials uniquely. In fact, by varying values of V_0 , V_1 , W_0 , and W_1 from the values for a reasonable fit, we have obtained a range of acceptable values for the reaction 155-MeV $\text{C}^{12}(p,2p)\text{B}^{11}$. The s - and p -state locations could be reasonably reproduced with the values of V_0 in the range 12 to 36 MeV if V_1 has the appropriate value in the range 30 to 50 MeV. The s -state magnitude was approximately reproduced with very widely different pairs of values for W_0 and W_1 ; 24 MeV, 18 MeV and 40 MeV, 12 MeV, while in the p -state case the values were 24 MeV, 32 MeV, and 40 MeV, 24 MeV. Thus we do not attach much significance to the values obtained from curve fitting. The method we employed in obtaining fits is as follows: First, the correlations were computed using the values given by Berggren and Jacob,¹² who had computed these values via the method of Kerman, McManus, and Thaler assuming the proton energies to be 70 and 170 MeV. The locations and magnitudes of both the p - and s -state curves were not very well reproduced using equal values of the optical potentials as had also been done by Berggren and Jacob¹² in a semiclassical approximation. To obtain reasonable fits then, only the parameters of the outgoing

particles had to be varied. They were found to be unequal for the s - and p -state correlations.

An estimate of the strength V_s of the two-body delta-function interaction potential was obtained by roughly reproducing the absolute magnitude of the cross sections. However, the value of V_s obtained is not unique but is dependent on the sets of W_0 and W_1 used to fit the data. Our value of 800 MeV F^3 is consistent with the values found by Agodi and Schiffrer¹⁸ from the $\text{Si}^{28}(p,n)$ reaction, and is approximately twice that for free n - p scattering with a delta-function interaction.

Computing costs made it uneconomical for us to perform a DWBA calculation with a finite range interaction potential. In the plane-wave Born approximation the effect on the angular correlation of a finite-range potential is to decrease the cross section at larger angles relative to that at smaller angles.

Surface localization in the $\text{C}^{12}(p,2p)\text{B}^{11}$ reaction was investigated by evaluating the radial-overlap integrals over the region outside of a cutoff radius. It was found that the region inside the alpha-particle rms radius does not contribute appreciably to the p -state cross section at both 40- and 155-MeV incident energies.

Thus even with the error in the present experimental data, $(p,2p)$ angular correlations provide some useful information on nuclear structure. However, to obtain any more information it is absolutely necessary to greatly improve the present energy and angular resolution, as our analysis has shown that even an unequal energy sharing of 10 MeV between the emergent protons is enough to smear out the angular correlation features.

ACKNOWLEDGMENTS

We are grateful to Dr. T. Berggren, Dr. G. Jacob, Dr. A. Agodi, and Dr. G. Schiffrer for prepublication information and to Dr. C. A. Hurst and K. A. Amos for helpful discussions and criticism.